# Enhanced Model of Turbulence for the Design of Optical Satellite Systems

Tituan Allain[1,2], Rajiv Boddeda[1], Sylvain Almonacil[1], Daniel Romero Arrieta[1], Sébastien Bigo[1]

[1] Nokia Bell Labs, 7 Route de Villejust, 91620 Nozay, France, tituan.allain@nokia.com
[2] Institut d'Optique Graduate School, Paris-Saclay University, 2 Av. Fresnel, 91120 Palaiseau, France

**Abstract** *We develop a model which accurately predicts the spatio-temporal variation of atmospheric turbulence effects across the optical beam of a free space optical link. We show that, in some conditions, the required optical launched power can be reduced by 2 dB, particularly at low windspeed.*

## Introduction

Free space optical links are sensitive to meteorological conditions such as air turbulence. With turbulence, the spatial refractive index of the transmission medium becomes irregular and impacts the optical beam wavefront. Occasionally, the spatial phase fluctuations translate into optical received power drops below the threshold needed for data demodulation during a certain period known as fading duration[1]. Consequently, the link availability or throughput is reduced. Fading statistics are often not available and thus need to be generated numerically for different weather conditions and locations. Imprecise predictions would lead to over or under dimensioning the mitigation mechanisms and to implement unnecessary design margins. The typical approach to model the impact of turbulence on beam propagation is to divide the atmosphere into several layers parallel to the ground and to compute the refractive index variations in each layer (referred to as phase screen). To model the turbulence evolution in the line of sight over time, current models only consider the translation of layers due to the wind but discard the evolution of the turbulence state within each eddies of the layer. This hypothesis is referred to as Taylor's "frozen" turbulence[2].

In this work, we propose to amend the existing models by accounting for the impact of the turbulence eddies evolution[3-4]. Our model uses the field measurements to realistically account for the dissipation of the eddies[5]. The paper is organized as follows. Firstly, we describe our methodology to simulate an optical link between the ground and a geostationary satellite. Secondly, we compare our simulation results with the data from a measurement campaign at Tenerife[6]. Finally, we illustrate how the power fadings can differ with and without the temporal evolution of the eddies in the example of a typical low wind speed[7] and strong turbulence[8] scenario and show how to derive the impact on the required optical launched power.

## Principle of the numerical simulation

Fig. 1 schematizes how turbulence evolves within one layer of the atmosphere at different wind speeds. The frozen flow approximation considers that the phase screens are "frozen" in time, while they are moved across by the wind. This hypothesis is valid at high windspeeds (~5 m/s at ground level) because any evolution of the turbulence eddies is slower than the time needed for the air cells to move cross the beam spot (Fig. 1a). At low wind speeds (Fig. 1b), this approach fails as the evolution of the turbulence eddies is no longer negligible.

In our simulations, we generate several turbulent layers and then use the split-term propagation method[9,10] to compute the propagation of a light beam through the consecutive layers of turbulent atmosphere. Each time the beam encounters a layer, its wavefront is modified by the turbulent phase screen, and then it propagates to the next layer. For each layer, the 2D spatial spectrum of the phase $\tilde{\varphi}$ is generated in the Fourier spatial domain using Eq. (1).

$$\tilde{\varphi}(\vec{\kappa}) \propto \sqrt{PSD(\vec{\kappa})} \cdot N(\vec{\kappa}) \quad (1)$$

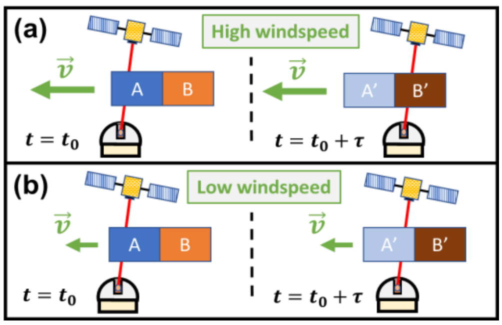


**Fig.1***:* Turbulence evolution. **a)** At high windspeed the correlation time $\tau$ of the turbulent cells A and B is much longer than their travel time. State A'(≠A) will not be reached before B falls in the line of sight. **b)** at low windspeed, the correlation time $\tau$ of the turbulent eddies A and B is comparable to the travel time. State A evolves to A' before B is in the line of sight. Self-evolution of the eddies cannot be neglected as it is in the frozen flow approach.

978-1-6654-3868-1/21/$31.00 ©2021 IEEE

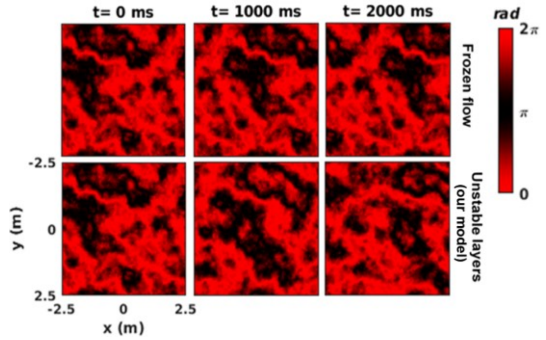


**Fig.2:** Example of a phase screen being translated at the wind speed based on the frozen flow approach *(top)* or being translated and evolving by itself *(bottom)*. The wind blows from the left to the right of the figure at 1 m/s.

Where $\vec{\kappa}$ is a spatial frequency sampled over the 2D plane, the phase power spectral density (PSD) is obtained with the Van Karman model and $N(\vec{\kappa})$ is a randomly generated complex Gaussian value, with unitary variance for each $\vec{\kappa}$. With frozen flow, each phase screen is translated horizontally at the wind speed $\vec{v}$ of each layer. Hence, the $N(\vec{\kappa})$ samples calculated from Eq. (1) are multiplied in the Fourier space by a phase term using Eq. (2) to obtain the translation between time samples $t_i$ and $t_{i+1} = t_i + \Delta t$.

$$N_{t_{i+1}}(\vec{\kappa}) = N_{t_i}(\vec{\kappa}) \cdot e^{-i\vec{\kappa}\cdot\vec{v}\Delta t} \qquad (2)$$

In our approach, we use Eq. (3) to introduce a time-dependence of the $N(\vec{\kappa})$ values, according to a Markov process[3,4]. The wind translation is still applied in the Fourier space, but for each spatial frequency $\vec{\kappa}$ a new random value $X(\vec{\kappa})$ is added to $N(\vec{\kappa})$ with a correlation time $\tau(\vec{\kappa})$.

$$N_{t_{i+1}}(\vec{\kappa}) = e^{-\Delta t/\tau(\vec{\kappa})} \cdot N_{t_i}(\vec{\kappa}) \cdot e^{-i\vec{\kappa}\cdot\vec{v}\Delta t} + \sqrt{1 - e^{-2\Delta t/\tau(\vec{\kappa})}} \cdot X(\vec{\kappa}) \qquad (3)$$

The value of $\tau(\vec{\kappa})$ is set arbitrarily in existing methods[4], whereas we use the dissipation rate of the turbulent cells $\varepsilon$ in Eq. (4) to calculate it[3,11].

$$\tau(v,\kappa) = \varepsilon(v)^{-1/3}\kappa^{-2/3} \qquad (4)$$

$\varepsilon$ is measured in situ with a sonic anemometer or LIDAR and depends on weather, altitude, and wind speed[5]. From Eq. (4), the smaller the eddies, the quicker they decorrelate over time (lower $\tau$) as they correspond to higher spatial frequencies. A typical phase screen movement due to wind using the frozen flow and our approach is illustrated in Fig. 2. The translation of the phase screen with the horizontal movement of the wind can clearly be seen in frozen flow conditions, whereas additional phase changes can be seen when emulating the evolution of eddies.

Even though the model described in this paper can be used to simulate both up and downlinks, this paper focuses on uplinks for which the efficiency of adaptive optics, which is the main mitigation technique for ground-satellite links, is limited. However, the simulation of the downlink propagation is much simpler to compute than an uplink simulation because the distorted wave profile needs to be computed only in the atmosphere (~20 km), and not over the entire propagation distance (>1000 km). Hence, we use the reciprocity principle[10] to calculate the coupling coefficient of the uplink beam into the satellite telescope by retro propagating a beam from the satellite to the ground. In our simulation tool, we emulate an adaptive optics-based phase pre-compensation system for geostationary satellites[10,12]. It uses the readings issued from the adaptive optics of the downlink by applying the opposite phase distortion to the uplink. However, despite this pre-compensation, the fadings cannot be fully mitigated due to the point ahead angle of 18 µrad between the downlink and the uplink beams, which makes the two beams travel through slightly different paths. Our model is designed to reproduce these residual fadings.

**Parameters of the simulation**

In our simulations, the atmosphere is divided into ten independent layers. Their successive thickness is increased quadratically with altitude to consider the higher impact of low-altitude layers due to higher pressure and to the thermal radiation of the ground. We use the Hufnagel-Valley profile[1,13] to characterise the turbulence strength from the ground up to 20 km altitude and neglect the impact of turbulence above. We then incorporate the time dependence of the turbulence using our model. For simplicity, we assume that $\varepsilon$ depends only on the wind speed $v$ and does not vary with altitude, but one could incorporate these variations in the model if needed. We use two types of median profiles $\varepsilon$, corresponding respectively to a stable and unstable atmosphere, as extracted from[7]. Concisely, a stable atmosphere corresponds to a slow evolution of the turbulence eddies (small $\varepsilon$ and large $\tau$) while it is the opposite for an unstable

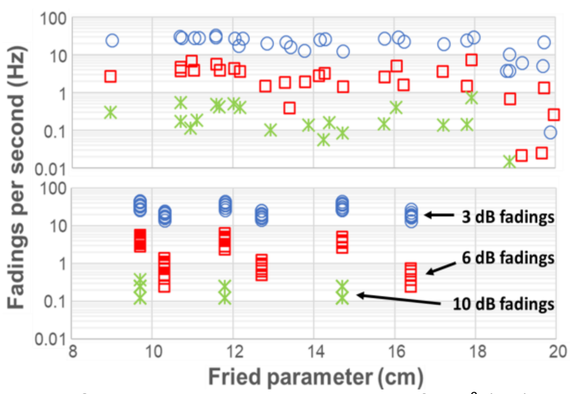


**Fig.3:** Comparison between experimental from [6] (top) and simulated data (bottom) for an uplink transmission to a geostationary satellite.

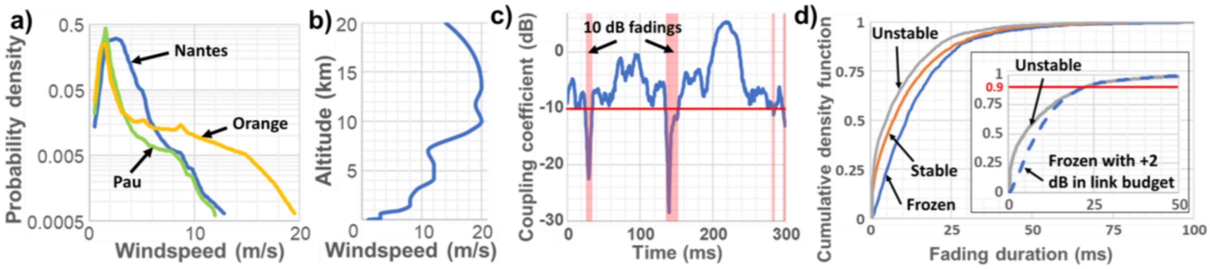


**Fig. 4:** ***a)*** Distribution of winds extracted from [7] for the cities of Nantes, Pau and Orange ***b)*** Wind profile that was used for the simulation ***c)*** 300 ms long time series of the simulated coupling coefficients in the fibre for an uplink transmission ***d)*** Cumulative density function of the 10 dB fading durations for the frozen flow scenario and in the stable and unstable profiles using our approach ***(inset)*** Cumulative density functions for the unstable scenario, and for frozen flow with additional 2 dB budget.

atmosphere. For each wind profile, we compute turbulence time series sampled at 2 kHz.

In the literature experimental measurements for uplink data transmission are scarce. In [6], a telescope diameter of 5 cm is used. With such a small beam size, the impact of the self-evolution of the turbulent eddies is negligible and we do not expect any difference between the prediction of frozen flow and our approach. Nevertheless, we use this scenario to check the consistency of our approach in the regime where the frozen flow hypothesis is valid. Fig. 3 (top) shows the fading frequencies from [6]. The Fried parameter on the x axis represents the phase correlation length at the receiver and quantifies the turbulence strength, i.e. a smaller Fried parameter indicates stronger turbulence. The measurements were performed on an uplink between a ground station in Tenerife and the Alphasat geostationary satellite operating at 1.06 µm laser wavelength during a four-day survey. Fig. 3 (bottom) shows the simulation results, revealing a good agreement with the experimental data. We were also able to accurately recreate scintillation indexes, fading durations, and fading frequencies by extracting the wind speeds from the meteorological data and setting the ground wind speeds to $v \in [1, 10]\, m/s$, and adjusting the parameter $W \in [22, 38]\, m/s$ from the Hufnagel-Valley profile.

### Impact on future satellite optical links

Next generation optical satellite systems will use larger beam diameters to reduce geometrical propagation losses, typically >20 cm, so we extend the use of our model under this condition. We simulate a 1.5 µm wavelength uplink transmission. To extract the most likely example of wind profile, we reviewed the windspeed probability distributions over three different French cities namely Orange, Pau, and Nantes, reported in[7]. We observe a peak in the range 2-3 m/s. Therefore, we feed our model with the example profile of Fig. 4b from meteorological data, which happens to fall in this range. It corresponds to a typical scenario of anticyclonic weather: 2 m/s wind speed at the ground level and 20 m/s in the tropopause. We consider a day with strong turbulence, i.e. when the temperature gradients at ground level are large, which can be characterized by a typical[8] structure constant of the refractive index at the ground level $C_n^2 = 10^{-13}\, m^{-2/3}$. Under these conditions, we evaluate the received optical power timeseries using our approach and Frozen flow. Even though our approach could generate infinitely long time series, for proper comparison with the frozen flow approach, we generate 50 series of 4 s using both methods. In Fig. 4c, we show 300 ms of received optical power series which exhibits fluctuations over several tens of dB. For a system with 10 dB margin, a fading occurs if the power falls below - 10 dB. In Fig. 4d, we plot the cumulative density functions of the fading durations from the complete set of series. The frozen flow approach overestimates the fading durations. Should a system designer ensure that 90% of the fading events last for less than a given duration, then Fig. 4d inset shows that the frozen flow assumption predicts 2 dB more link margin than necessary, and thus additional launched power. Interestingly, the shorter but more frequent fading events seen with our model can be mitigated more efficiently with any given time-diversity correction codes, which should result in further budget reduction[14]. Furthermore, when the atmosphere becomes more stable and the evolution of turbulence eddies is slower, Fig. 4d suggests that our model converges to the predictions of the frozen flow model, as confirmed by further simulations not reported here.

### Conclusion

We enriched the state-of-the-art turbulence models by accounting for turbulent eddies evolution. We verified that our simulations were able to reproduce the experimental observations. At low windspeeds, significant differences between the frozen flow and our approach were observed. The former approach consistently overestimated the likelihood of long fading events which steer in the direction of over dimensioned optical power budget. Hence, we believe that this new approach is better suited to help design optical links in the worst-case turbulences.

## References


[1] H. Kaushal and G. Kaddoum, "Optical Communication in Space: Challenges and Mitigation Techniques," in IEEE Communications Surveys & Tutorials, vol. 19, no. 1, pp. 57-96, (2017).

[2] Taylor G. I. The Spectrum of Turbulence Proc. R. Soc. A.164476–490, (1938).

[3] H. Gingsjö, "Modeling and Simulation of Tropospheric Water Vapour with Gaussian Random Fields", master thesis (2018).

[4] S. Srinath, et al., "Computationally efficient autoregressive method for generating phase screens with frozen flow and turbulence in optical simulations", Opt. Express 23(26), 33335-33349 (2015)

[5] N. Bodini, et al., "Estimation of turbulence dissipation rate and its variability from sonic anemometer and wind Doppler lidar during the XPIA field campaign", Atmos. Meas. Tech. 11, 4291–4308, (2018).

[6] K. Saucke, et al., "Three years of optical satellite to ground links with the T-AOGS: data transmission and characterization of atmospheric conditions," Proc. SPIE 11180, International Conference on Space Optics — ICSO 2018, 111801D (2019).

[7] Drobinski, P., Coulais, C. & Jourdier, B. Surface Wind-Speed Statistics Modelling: Alternatives to the Weibull Distribution and Performance Evaluation. Boundary-Layer Meteorol 157, 97–123 (2015).

[8] J. A. Nessel and R. M. Manning, "Derivation of Microwave Refractive Index Structure Constant (C2n) of the Atmosphere From K-Band Interferometric Phase Measurements," in IEEE Transactions on Antennas and Propagation, vol. 62, no. 11, pp. 5590-5598, (2014).

[9] J. M. Martin and S. M. Flatté, "Intensity images and statistics from numerical simulation of wave propagation in 3-D random media," Appl. Opt. 27, 2111-2126 (1988).

[10] C. Robert, J.-M. Conan, and P. Wolf. "Impact of turbulence on high-precision ground-satellite frequency transfer with two-way coherent optical links". Phys. Rev. A, 93(3), 033860 (2016).

[11] Glenn Flierl, and Raffaele Ferrar, "12.820 Turbulence in the Ocean and Atmosphere, Chap. 5. Spring 2007". MIT OpenCourseWare, https://ocw.mit.edu, Creative Commons BY-NC-SA.

[12] Nicolas Védrenne et al "Adaptive optics pre-compensation for GEO feeder links: towards an experimental demonstration", in Space Optical Systems and Applications (ICSOS 2017), IEEE (2017).

[13] R.E. Hufnagel, "Propagation through atmospheric turbulence", The Infrared Handbook, Chap. 6. USGPO (1974).

[14] Chien-Chung Chen "Uplink channel coding for ground-to-space optical links (Conference Presentation)", Proc. SPIE 10910, Free-Space Laser Communications XXXI, 109101A (2019).